
Knowledge Representation Combining Quaternion Path Integration and Depth-wise Atrous Circular Convolution

Xinyuan Chen^{1,2}

Zhongmei Zhou¹

Meichun Gao¹

Daya Shi¹

Mohd Nizam Husen²

¹School of Technology, Fuzhou Technology and Business University, Fuzhou, Fujian, China

²Malaysian Institute of Information Technology, Universiti Kuala Lumpur, Kuala Lumpur, Malaysia,

Abstract

Knowledge models endeavor to improve representation and feature extraction capabilities while keeping low computational cost. Firstly, existing embedding models in hypercomplex spaces of non-Abelian group are optimized. Then a method for fast quaternion multiplication is proposed with proof, with which path semantics are computed and further integrated with the attention mechanism based on the idea semantic extraction of relation sequences could be regarded as a multiple rotational blending problem. A depth-wise atrous circular convolution framework is set up for better feature extraction. Experiments including Link Prediction and Path Query are conducted on benchmark datasets verifying our model holds advantages over state-of-the-art models like Rotate3D. Moreover, the model is tested on a biomedical dataset simulating real-world applications. An ablation study is also performed to explore the effectiveness of different components.

1 INTRODUCTION

Knowledge Graph (KG) is composed of structured fact triples. Entities in the triples are represented as nodes in the graph and the relations between head and tail entities are represented as edges connecting the nodes. KGs are widely applied in areas such as question answering [Hao et al., 2017] and personalized recommendation [Guo et al., 2020]. However, existing KGs are incomplete and contain noise. One of the ideas is to embed entities / relations into low-dimensional vector spaces and apply KG completion techniques to predict missing facts. For example, in RotatE [Sun et al., 2019] relations are mapped as rotations and the distances between the head vectors after rotations and the tail vectors are utilized to determine whether triple facts

are true. However, different KGs contain various proportions of multiple relation modes including Symmetry, Anti-symmetry, Inversion and Composition. Different models are capable of learning representations for different modes and so far there is no perfect embedding solution.

Most of existing embedding models learn representations in the two smallest domains of Divisor Algebra, \mathbf{R} and \mathbf{C} . With Quaternion algebra \mathbf{H} and Octonion algebra \mathbf{O} models could develop higher expressivity with less parameters; what's more, the characteristic of non-commutative law in non-Abelian groups helps to model the compositional relation mode. Three-dimensional (3D) and four-dimensional (4D) spatial embeddings with quaternions are adopted in Rotate3D [Gao et al., 2020] and QuatE [Zhang et al., 2019] respectively. Subsequent models enhance expressivity by adding entity / relation-specific quaternions or increasing embedding dimensions; larger parameter scales as well as limited feature extraction capabilities leave space for improvement.

Semantic information carried by relation paths between entity pairs helps to determine the validity of triples in knowledge inference. Many models employ frameworks including Recurrent Neural Network (RNN) [Jozefowicz et al., 2015], Long Short-Term Memory (LSTM) [Greff et al., 2016][Zhou et al., 2016] and Gated Recurrent Unit (GRU) [Lu and Duan, 2017] to merge vector sequences while the computational efficiency could be further boosted.

ConvE [Dettmers et al., 2018] performs 2-dimensional (2D) reshaping on concatenation matrices to enhance interactions and extracts deep non-linear features with Convolutional Neural Network (CNN). InteractE [Vashishth et al., 2020] adopts an optimized reshaping strategy as well as the circular convolution. In order to capture rich features of complex relations, inspired by neurons with different sizes of receptive fields, Atrous Convolution [Chen et al., 2017] expands the fields for larger interaction spaces while maintaining parameter scales. Moreover, introduction of the attention mechanism to integrate features extracted by

kernels with various sizes helps to stabilize model performance. The strategies above are jointly applied in our study.

APAC (A Knowledge Representation Model based on the Non-Abelian groups, Path Semantics and Depth-wise Atrous Circular Convolution) is proposed and main work includes:

1. A hypercomplex embedding model with improved score function and loss function designs is brought forward based on state-of-the-art (SOTA) quaternion models, in which Quaternion algebra, a Hamilton group with the smallest order is employed to learn multiple relational modes between entities. Embedding is also extended to the octonion space.
2. Based on the idea of multi-hop reasoning in Rotate3D, a fast multiplicative calculation method for quaternion sequences is proposed with proof for rapid feature mergers of relational paths which are then integrated with the attention mechanism.
3. A depth-wise atrous circular convolution framework is set up to enhance the feature extraction capability.
4. Experiments including Link Prediction and Path Query are carried out on benchmark and industry datasets to verify model effectiveness. Ablation study is further performed (see supplementary materials).

2 RELATED WORK

Embedding models could be roughly divided into translation/rotation-based distance models and similarity-based semantic models.

TransE [Bordes et al., 2013], a distance model, maps the relations to translation vectors. TransE holds that if a triple is valid, the head vector after translation should be close to the tail, denoted as

$$\mathbf{h} + \mathbf{r} \approx \mathbf{t}, \quad (1)$$

where \mathbf{h} , \mathbf{r} , \mathbf{t} are the vector representations of the head entity, the relation and the tail entity respectively. L1 / L2 distance between vectors is taken as the score of the triple and a margin-based loss function is applied. With simple structure TransE achieves brilliant performance; however, it lacks the ability to learn symmetric relational representations. Most subsequent models improve by adding dimensions or expanding mapping spaces [Wang et al., 2014][Lin et al., 2015] followed by initiatives employing sparse matrix decomposition [Ji et al., 2016] to reduce the number of parameters. RotatE models relations as 2D rotations from head to tail entities in complex spaces with Hadamard product and normalized constraints. The calculation complies with the commutative law. Therefore, RotatE may not perform well on non-commutative relational modes (e.g., Adam’s father’s wife is not Adam’s wife’s father).

RESCAL [Nickel et al., 2015], an early semantic model,

calculates the factorization of third-order adjacency tensors as triple scores. RESCAL holds strong expressivity but high complexity makes it difficult to train. DistMult [Yang et al., 2014] represents the relations as diagonal matrices to simplify calculations, capable of learning the symmetric and inverse modes. ComplEx [Trouillon et al., 2016] further extends the embedding to complex spaces to enhance the learning ability for anti-symmetric patterns. Hermitian product is used to calculate triple scores and reduce the number of parameters; however, it is still difficult for ComplEx to learn the non-commutative pattern. Lacroix et al. [2018] upgrade ComplEx with L3 regularization and a multi-class log loss.

Since hypercomplex spaces of non-Abelian groups hold strong expressivity and quaternion / octonion calculations are rather efficient, some models expand mapping spaces with them in recent years. Hyperbolic spaces are also taken into consideration [Chami et al., 2020].

QuatE represents relations as rotations in 4D spaces with quaternions to provide more degrees of freedom while avoiding Gimbal Lock. QuatE first calculates the Hamilton product between the head quaternion Q_h and the unit relation quaternion \hat{W}_r , and then calculates the inner product of the result with the tail quaternion Q_t so as to obtain the triple score. Compared with real/complex space models, QuatE could also learn symmetric (set the coefficients of imaginary parts to 0), anti-symmetric (conjugate quaternion), and inverse (coefficients set to -1) relation modes while enjoying larger spaces, less parameters and lower computational cost. On such basis, QuatDE [Gao et al., 2021], QuatRE [Nguyen et al., 2020] and DualE [Cao et al., 2021] further enhance the expressivity by increasing dimensions or adding quaternions, though limiting model scalability.

Most models above ignore rich semantic information contained in relation paths [Wang et al., 2016]. Lao et al. [2011] generate paths with the Random Walk algorithm and verify path values in knowledge inference. However, early studies take paths as atomic features, leading to huge feature matrices [Shang et al., 2019]. Neelakantan et al. [2015] and Das et al. [2016] decompose the paths into relation sequences and input them into RNN, reducing computational cost with parameter sharing. Nonetheless, the possibility that multiple paths to different extents associate with the candidate relations is ignored [Xie et al., 2017]. To solve this, Jiang et al. [2017] introduces the attention mechanism. Rotate3D models path-based multi-hop reasoning as multiple rotations and in our study a calculation method for fast rotation blending and integration is proposed.

Another vital indicator of knowledge representation models is feature extraction capability besides expressivity and computational overhead. Parameters in CNN are much less than those in fully connected neural networks and are

widely employed in Natural Language Processing in recent years. Compared with distance models, 2D convolution in ConvE is able to enhance interactions between entities/reasons and extract richer features for embedding learning [Balažević et al., 2019a]. However local features are partly lost since ConvE leaves out translational/rotational attributes. Vashishth et al. [2020] believe that both the distance and semantic models could only capture shallow features, so they propose Checkered Reshaping and Circular Convolution to improve interactions. On this basis, Wang et al. [2021] suggest the multi-size atrous convolution combined with the attention mechanism could bring similar effects.

Therefore, in our model hypercomplex embedding is employed with optimization. Path semantics are extracted and integrated by fast rotational blending calculation and the attention mechanism. Also a depth-wise atrous circular convolution is defined to facilitate feature extraction.

3 APAC FRAMEWORK

As is shown in Figure 1, APAC learns entity / relation embeddings in hypercomplex spaces. A fast relational path multiplication calculation is designed and the attention mechanism is introduced to integrate path semantics. The feature extraction capability is further enhanced with the depth-wise atrous circular convolution.

3.1 HYPERCOMPLEX EMBEDDING

Relation representations as rotations of 3D vectors in 3D subspaces of 4D spaces with quaternion embedding could effectively model multiple relational modes. QuatE’s inner product score function is mostly used to solve logistic regression problems while distance-based score functions with L1 / L2 norm and margin-based normalized loss functions perform better with noise. Therefore, the Hamilton product between the head Q_h and the relation r is firstly calculated, and then the distance between the result and the tail Q_t is computed. The score function for quaternions is denoted as

$$\phi(\mathbf{h}, \mathbf{r}, \mathbf{t}) = \|\mathbf{h} \otimes \mathbf{r} - \mathbf{t}\|. \quad (2)$$

Accordingly, the loss function is defined as

$$L = -\log \sigma(\gamma - \phi(\mathbf{h}, \mathbf{r}, \mathbf{t})) - \sum_{i=1}^m p(\mathbf{h}'_i, \mathbf{r}, \mathbf{t}'_i) \log \sigma(\phi(\mathbf{h}'_i, \mathbf{r}, \mathbf{t}'_i) - \gamma) + \lambda_1 \|\mathbf{Q}\|_2^2 + \lambda_2 \|\mathbf{R}\|_2^2, \quad (3)$$

consulting the self-adversarial negative sampling in RotatE, where σ is the Sigmoid function, γ is the margin with a slack coefficient [Nayyeri et al., 2020], $(\mathbf{h}'_i, \mathbf{r}, \mathbf{t}'_i)$ refers to the i th invalid triple, m is the total number of invalid triples, λ_1, λ_2 are the coefficients for L2 norm en-

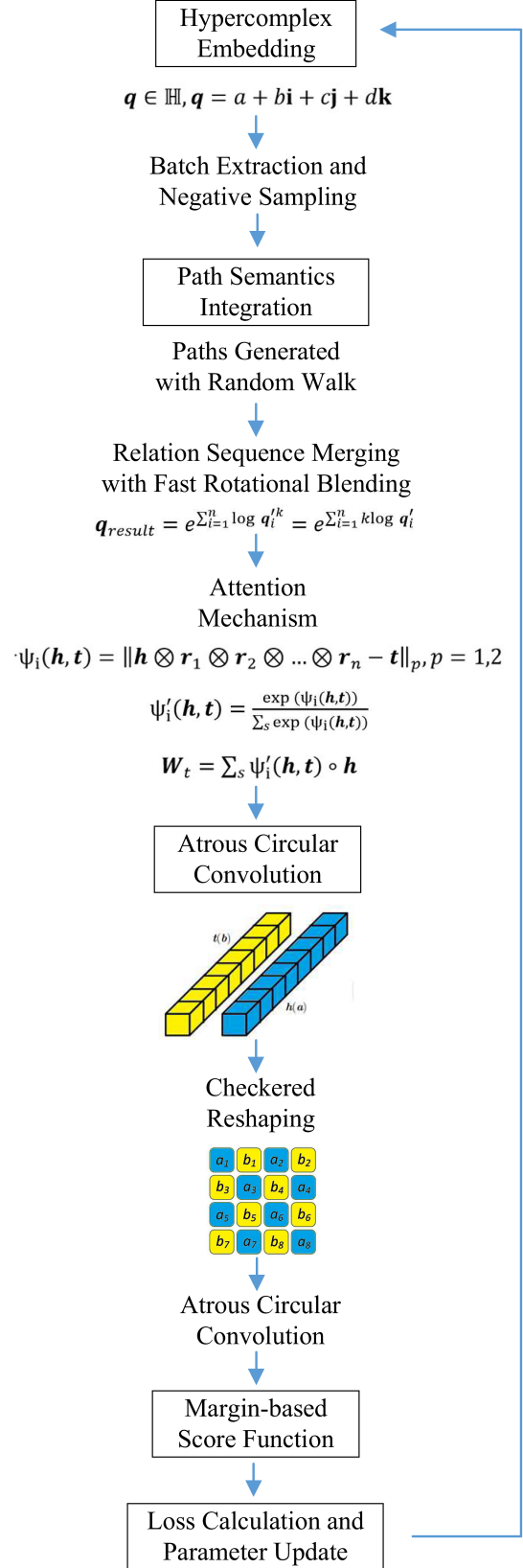


Figure 1: Framework of APAC.

tity/relation constraints, $p(\mathbf{h}'_i, \mathbf{r}, \mathbf{t}'_i) = \frac{\exp \beta f(\mathbf{h}'_i, \mathbf{t}'_i)}{\sum_{i=1}^m \exp \beta f(\mathbf{h}'_i, \mathbf{t}'_i)}$ calculates the probability distribution of negative sampling, β is the sampling temperature, and $f(\mathbf{h}'_i, \mathbf{t}'_i) = -\phi(\mathbf{h}'_i, \mathbf{t}'_i)$.

Similarly, the score function and loss function for octonions is defined similarly.

Since overall constraints are already imposed on \mathbf{Q} and \mathbf{R} , the unit constraint on the relational quaternions seems unnecessary, compressing the entity rotation spaces and weakening expressivity. L1 normalization helps to generate sparse representations and only retain key features so as to reduce noise interference, but data could be left out on valuable channels. It is found that L2 constraint performs better in experiments.

3.2 EXTRACTION AND INTEGRATION OF PATH SEMANTICS

Following the path query solution proposed by Gao et al. [2020] based on multi-hop reasoning, in our study the multi-hop reasoning is regarded as continual Hamilton products of relational sequences taking advantages of the non-commutative characteristic of quaternions. For such calculation, a fast path feature extraction and the integration method is proposed.

Firstly, multiple paths are generated between entities with Random Walk and encoded as quaternion relation sequences. Length of path is defined as the number of relations in the path. Allow different length but set an upper threshold. Path feature extraction could be taken as multiple rotational blending. The operation space for rotations is non-linear and it is not right to directly add the rotational quaternions together.

Theorem 1: For a quaternion sequence, $\mathbf{q}_1, \mathbf{q}_2, \dots, \mathbf{q}_i, \dots, \mathbf{q}_n, i = 1, 2, \dots, n$, the continual Hamilton product could be calculated as

$$\mathbf{q}_{\text{result}} = e^{\sum_{i=1}^n \log q_i^k} = e^{\sum_{i=1}^n k \log q_i^k}. \quad (4)$$

Please see Appendix A for Proof and Illustration. Path score is denoted as

$$\Psi_i(\mathbf{h}, \mathbf{t}) = \|\mathbf{h} \otimes \mathbf{r}_1 \otimes \mathbf{r}_2 \otimes \dots \otimes \mathbf{r}_n - \mathbf{t}\|_p, p = 1, 2. \quad (5)$$

In order to reduce noise and extract key features, the attention mechanism is introduced to integrate path representations. denoted as

$$\Psi'_i(\mathbf{h}, \mathbf{t}) = \frac{\exp(\phi_i(\mathbf{h}, \mathbf{t}))}{\sum_s \exp(\phi_i(\mathbf{h}, \mathbf{t}))}, \quad (6)$$

in which s is the path set. The Softmax function is employed to normalize path scores. Structured representation

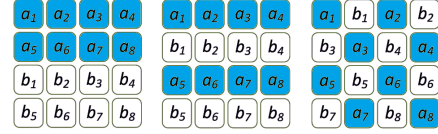


Figure 2: Stacked (left), Alternate (middle) and Checkered Reshaping (right).

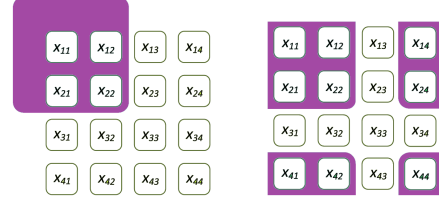


Figure 3: Ordinary Convolution (left) and Circular Convolution (right).

from path semantics of the tail entity is

$$\mathbf{W}_t = \sum_s \psi'_1(\mathbf{h}, \mathbf{t}) \circ \mathbf{h}. \quad (7)$$

3.3 DEPTH-WISE ATROUS CIRCULAR CONVOLUTION

In this part the checkered reshaping and the depth-wise atrous circular convolution are combined to improve the model's capability in feature extraction.

The reshaping function is defined as $\pi : \mathbf{H}^k \times \mathbf{H}^k \rightarrow \mathbf{H}^{m \times n}$, where $m \times n = 2k$. The comparison of stacked, alternate and checkered reshaping is shown in Figure 2. Vashishth et al. [2020] argue that entity/relation interactions could be divided into two types, heterogeneous and homogeneous, denoted as $\mathcal{N}_{\text{het}}(\pi, k)$ and $\mathcal{N}_{\text{homo}}(\pi, k)$, $\mathcal{N}_{\text{het}}(\pi, k) + \mathcal{N}_{\text{homo}}(\pi, k) = 2 \binom{k^2}{2}$, $\mathcal{N}_{\text{het}}(\Omega_c(\pi), k)$ is with greater value in exploring entity/relation association. They prove that the proportion of $\mathcal{N}_{\text{het}}(\pi, k)$ is the highest with the checkered reshaping. Therefore, such strategy is applied.

Comparison between the ordinary convolution and the circular convolution is shown in Figure 3. Vashishth et al. [2020] believe $\mathcal{N}_{\text{het}}(\Omega_c(\pi), k) \geq \mathcal{N}_{\text{het}}(\Omega_0(\pi), k)$ where Ω_c is the circular convolution and Ω_0 is the ordinary convolution. The former is employed in our study, defined as

$$[\mathbf{I} \star \boldsymbol{\omega}]_{u,t} = \sum_{i=-\lfloor p/2 \rfloor}^{\lfloor p/2 \rfloor} \sum_{j=-\lfloor p/2 \rfloor}^{\lfloor p/2 \rfloor} \mathbf{I}_{[u-i]_m, [t-j]_n} \boldsymbol{\omega}_{i,j}, \quad (8)$$

where $\mathbf{I} \in \mathbf{H}^{m \times n}$, $\boldsymbol{\omega} \in \mathbf{H}^{p \times p}$ and $\lfloor \cdot \rfloor$ is the floor function. The depth-wise convolution extracts feature information channel by channel before mergers.

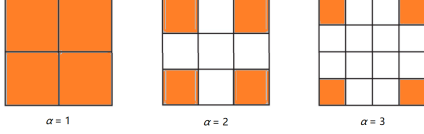


Figure 4: Convolution Kernels with Different Void Rates.

Wang et al. [2021] suggest that while single-size kernels benefit from parameter sharing and low computing overhead, their receptive fields are limited. On the contrary, the multi-size circular convolution with the attention mechanism could better extract critical features, so in this study the atrous convolution is employed. with the equivalent kernel size defined as

$$p' = p + (p - 1)(\alpha - 1), \quad (9)$$

where p is the size of a standard kernel, and α is the void rate. Holes are filled with 0, so the receptive field is enlarged with same number of parameters and same computational cost. Convolution kernels with different void rates are shown in Figure 4. . Given the number of kernels of each size C and feature matrix is $\pi(\mathcal{P}_k)$, features extracted by the j th ($j = 1, 2, \dots, C$) kernel of the i th ($i = 1, 2, 3$) size are denoted as

$$\mathbf{V} = \mathbf{f} \left(\pi(\mathcal{P}_k) \text{conv}(\omega_i^j) + \mathbf{b}_i \right), \quad (10)$$

where \mathbf{b}_i is the bias and $\mathbf{V}_1, \mathbf{V}_2, \mathbf{V}_3 \in \mathbf{R}^{C \times 2m \times n}$.

In order to reduce noise and highlight key features, the attention module is introduced to adaptively adjust the weights of features from various kernels. With convolution the score function is modified, denoted as

$$\phi(\mathbf{h}, \mathbf{r}, \mathbf{t}) = \frac{\|\text{conv}(\mathbf{h}, \mathbf{r}) \circ (\mathbf{h} \otimes \mathbf{r}) - \text{conv}(\mathbf{r}, \mathbf{t}) \circ \mathbf{t}\|}{\|\text{conv}(\mathbf{h}, \mathbf{r}) \circ (\mathbf{h} \otimes \mathbf{r}) - \text{conv}(\mathbf{r}, \mathbf{t}) \circ \mathbf{t}\|}. \quad (11)$$

where \circ denotes the Hadamard product and \otimes denotes the Hamilton product. The loss gradient of entity/relation embeddings could propagate bi-directionally through the convolution or hypercomplex multiplications.

4 EXPERIMENTS

4.1 LINK PREDICTION

Given an entity and a relation, the missing entity is predicted. The higher the ranking of correct triples in the candidate set are, the stronger the prediction capability of the model is. Mean Reciprocal Rank (MRR) and the proportion of correct entities / triples in the top N candidates (Hits@ N , $N = 1, 3, 10$) are selected as metrics. The higher the score, the better. Bernoulli method [Wang et al., 2014] is adopted to randomly replace entities to create invalid

Table 1: Dataset Statistics for Link Prediction.

Dataset	Entity	Relation	Degree	Train Set	Val. Set	Test Set
WN18RR	40943	11	2.283.6	86,835	3034	3134
FB15k-237	14541	237	19.7830	272,115	17535	20466
YAGO3-10	123182	37	9.688.7	1,079,040	5000	5000

triples. Filtered strategy is employed [Bordes et al., 2013]. Head and tail predictions are regarded as one task and the scores are combined.

Experiments are conducted on three benchmark datasets: WN18RR [Dettmers et al., 2018], FB15k-237 [Toutanova and Chen, 2015] and YAGO3-10 [Mahdisoltani et al., 2014]. WN18RR and FB15k-237 remove inverse relations to fix the high-score flaw. The relations in the YAGO3-10 dataset are mostly descriptive attributes about human. Some relations are with hierarchical structure, such as *hypernym* (WN18RR), *part-of* (FB15k-237) and *playsFor* (YAGO3-10). Dataset statistics are shown in Table 1, in which the degrees reflect the relational complexity of the datasets [Dettmers et al., 2018].

The following models are used as baselines: 1. TransE: Results from Ruffinelli et al. [2019]. 2. RotatE: Results from Sun et al. [2019]. 3. Rotate3D: Results from Gao et al. [2020]. 4. DistMult, ComplEx and ConvE: Results from Dettmers et al. [2018]. 5. ComplEx-N3: Results from Lacroix et al. [2018]. 6. QuatE: Results from Zhang et al. [2019]. We also make our own implementation and run on YAGO3-10, etc. (Codes are released on <https://gitee.com/tkgc/APAC>.) 7. ROTE/ATTE: embedding models in hyperbolic spaces, ATTE combining rotation and reflection while ROTE only containing rotation. Results from Chami et al. [2020]. 8. TUCKER: a SOTA semantic model with Tucker Decomposition. Results from Balažević et al. [2019b]. 9. CoKE: A SOTA path model employing Transformer to encode semantics. Results from Wang et al. [2019].

The Training details are in Appendix B. Results are shown in Table 2 taking a 5-time average. Results in bold indicate the best performance while those in italics are the second. APAC_q and APAC_o denote quaternion and octonion embedding respectively. It is obvious that the overall performance of APAC is better than mainstream models and APAC_q is significantly better than APAC_o at many indicators.

On WN18RR, the simplest dataset, Rotate3D and QuatE achieve best results while APAC_q secures the highest MRR and good Hits@1 Score. On the complex dataset FB15k-237, the advantages of APAC_q are more clear with highest MRR and Hits@1, 3. the Hits@1 score is 3.3% higher than that of QuatE while the Hits@10 score is catching up. On Yago3-10, the largest dataset, there is no comparison with Rotate3D (no available code), but APAC_q

Table 2: Link Prediction Results.

Model	WN18RR				FB15k-237				YAGO3-10			
	MRR	Hits@1	3	10	MRR	Hits@1	3	10	MRR	Hits@1	3	10
TransE	0.228	-	-	0.520	0.313	-	-	0.497	-	-	-	-
RotatE	0.476	0.428	0.492	0.571	0.338	0.241	0.375	0.533	0.495	0.402	0.550	0.670
Rotate3D	0.489	0.442	0.505	0.579	0.347	0.250	0.385	0.543	-	-	-	-
DistMult	0.430	0.390	0.440	0.490	0.241	0.155	0.263	0.419	0.340	0.240	0.380	0.540
ComplEx	0.440	0.410	0.460	0.510	0.247	0.158	0.275	0.428	0.360	0.260	0.400	0.550
ComplEx-N3	0.470	-	-	0.540	0.350	-	-	0.540	0.490	-	-	0.680
QuatE	0.482	0.436	0.499	0.572	0.366	0.271	0.401	0.556	0.502	0.428	0.543	0.674
ROTE	0.463	0.426	0.477	0.529	0.307	0.220	0.337	0.482	0.381	0.295	0.417	0.548
ATTE	0.456	0.419	0.471	0.526	0.311	0.223	0.339	0.488	0.374	0.290	0.410	0.537
TuckER	0.470	0.443	0.482	0.526	0.358	0.266	0.394	0.544	-	-	-	-
CoKE	0.484	0.450	0.496	0.553	0.364	0.272	0.400	0.549	-	-	-	-
ConvE	0.460	0.390	0.430	0.480	0.316	0.239	0.350	0.491	0.520	0.450	0.560	0.660
APAC _q	0.501	0.447	0.487	0.535	0.378	0.280	0.407	0.548	0.518	0.461	0.558	0.696
APAC _o	0.479	0.435	0.488	0.539	0.353	0.269	0.384	0.511	0.527	0.422	0.546	0.620

achieves highest or close to highest scores at all metrics, Hits@1 score 7.7% higher than that of QuatE and Hits@10 score higher than that of QuatE. APAC_o performs well at MRR and Hits@3. Comparison with Rotate3D and QuatE demonstrates that APAC holds strong learning ability for complex relational patterns which may come from the integration of path semantics or the depth-wise atrous circular convolution combined with the attention mechanism. Compared with TransE, DistMult, ComplEx, ROTE, ATTE and TuckER, APAC_q and APAC_o perform better indicating the effectiveness of hypercomplex embedding. APAC_q also holds certain advantages over CoKE, the SOTA context semantics model, verifying the forces of hypercomplex embedding and feature extraction methods. ConvE does not perform great due to the simple reshaping strategy. Follow-up experiments focus on APAC_q.

4.2 PATH QUERY

To verify model capabilities for modeling the composition pattern path query (multi-hop reasoning) is carried out following Rotate3D. Given the starting entity h and the path p , entities that h can reach via p are predicted and ranked. Two datasets provided by Guu et al. [2015] are employed, coming from WordNet and Freebase respectively. Dataset statistics are shown in Table 3. The same settings including the negative sampling and filtering strategy by Gao et al. [2020] are adopted. The average quantile (MQ) and Hits@10 are used as metrics. The higher the score, the better. Two training strategies are employed: only triples (denoted as Single) and all paths (Comp).

Best performance is achieved when the embedding dimension $d = 500$, batch size 512, learning rate $lr = 0.0005$, margin $\gamma = 8$ and other parameters same as on YAGO3-10.

Compare APAC with Bilinear [Guu et al., 2015], TransE, CoKE, RotatE and Rotate3D under the Single strategy, with ROP [Yin et al., 2018], using RNN to model paths), CoKE, RotatE and Rotate3D under the Comp strategy. Relevant results are from Gao et al. [2020] and the results are shown in Table 4, Table 5. It can be seen that except for the MQ score on WordNet, APAC_q-Single wins on all metrics in its group. APAC_q-Comp also achieves the highest or second highest scores for each indicator, and scores higher than APAC_q-Single, which is another proof APAC_q possesses the learning ability for the composition pattern and the ability to integrate path semantics. CoKE relies heavily on contexts, so it's a draw for CoKE and APAC_q-Comp under the Comp strategy. However, APAC_q-Comp performs much better under the Single strategy.

4.3 APPLICATION ON INDUSTRY DATASET

Domain-specific KGs are helpful for promoting knowledge application and the industry development. Apply our model to a biomedical dataset ogbl-biokg¹ containing 5 entity types including diseases, drugs, side effects, proteins and their functions as well as 51 relation types. The statistics is shown in Table 6. ogbl-biokg is collected from diversified sources with complex relation modes and broad confidence differences for facts, challenging models for extracting relation features and modeling knowledge uncertainty (another future plan). Random divisions of the train/val./test sets are made with proportions 94%, 3% and 3% respectively. Since the entity relations are rather dense and simply replacing the head or tail entity probably brings false negatives, replace the head and the tail entities at the same time to generate invalid samples with the ratio set to 1:1.

Best performance is achieved when the embedding dimen-

¹<https://ogb.stanford.edu/docs/linkprop/#ogbl-biokg>

Table 3: Dataset Statistics for Path Query.

Dataset	Entity	Relation	Train Set	Val. Set	Test Set	Train Paths	Val. Paths	Test Paths
WordNet	38551	11	110,361	2602	10462	2129539	11277	56477
Freebase	75043	13	316,232	5908	23733	6266058	27163	109557

Table 4: Path Query Results (Triple Training).

Model	WordNet		Freebase	
	MQ	Hits@10	MQ	Hits@10
Bilinear-Single	0.847	0.436	0.580	0.259
TransE-Single	0.837	0.138	0.862	0.454
CoKE-Single	0.731	0.157	0.730	0.367
RotatE-Single	0.937	0.479	0.833	0.453
Rotate3D-Single	0.941	0.494	0.894	0.547
APAC _q -Single	0.932	0.502	0.904	0.583

Table 5: Path Query Results (Path Training).

Model	WordNet		Freebase	
	MQ	Hits@10	MQ	Hits@10
ROP-Comp	-	-	0.907	0.567
CoKE-Comp	0.942	0.674	0.948	0.764
RotatE-Comp	0.947	0.653	0.901	0.601
Rotate3D-Comp	0.949	0.671	0.905	0.621
APAC _q -Comp	0.960	0.719	0.933	0.723

sion $d = 500, 1000$, batch size 512 and the learning rate $lr = 0.0001$, other parameters same as on YAGO3-10.

Compare APAC_q with TransE, DistMult, RotatE, QuatE, PairRE [Chao et al., 2020] and AutoSF+ [Zhang et al., 2021b]. The latter two are specially designed for modeling complex relations. PariRE introduces relationship-specific pair vectors for representation while in AutoSF+ an adaptive score function is proposed, pruning the search spaces with filters and predictors and replacing the greedy algorithm in AutoSF [Zhang et al., 2020] with Evolutionary Search.

Results are shown in Table 7. APAC_q performs best with slight differences between dimensions 500 and 1000, showing strong feature extraction capability under low dimensions. Translation / rotation models that only extract shallow features do not perform great and increasing dimensions does not bring obvious improvement. A similar situation occurs with QuatE. Compared with the semantic models, APAC_q holds obvious advantages. Compared with PariRE and AutoSF+, APAC_q upgrades performance without adding embedding or expanding the search spaces, which verifies the effectiveness of path semantic integration and our convolution framework.

It is worth noting that although additional path calculation and convolution operations are introduced, with the phased parallel training strategy, it only takes 1.5 hours for APAC_q to surpass QuatE’s best performance under dimension 500, which is only about 1/5 of the training time for the latter, indicating that our model improves feature extraction capability while boosting computing efficiency.

5 CONCLUSION

Compared with embedding models in real / complex spaces, a knowledge representation model with stronger expressivity and feature extraction capabilities is proposed with hypercomplex embedding, path semantic integration combining fast quaternion rotation blending and the attention mechanism, and the depth-wise atrous circular convolution. Low computational cost of quaternion multiplication, parameter sharing in CNN and phased parallel training strategy ensure rapid taking effect of the model on large datasets. Future work includes further improving on learning complex composition modes, applying Kronecker product to expand embedding spaces with high efficiency [Zhang et al., 2021a] and modeling knowledge uncertainty / time validity, etc.

A PROOF AND ILLUSTRATION OF THEOREM 1

Proof. For $q_1 \otimes q_2, q_2 \otimes q_1$, bisect the angles respectively, $q'_1 = q_1^{\frac{1}{2}}, q'_2 = q_2^{\frac{1}{2}}$, resulting in $q_1^{\frac{1}{2}} * q_2^{\frac{1}{2}} * q_1^{\frac{1}{2}} * q_2^{\frac{1}{2}}$ and $q_2^{\frac{1}{2}} * q_1^{\frac{1}{2}} * q_2^{\frac{1}{2}} * q_1^{\frac{1}{2}}$. Parts of the two calculations are the same. Further k -sect q_1, q_2 . The greater the value of k is, the higher the proportion of same calculations is. When $k \rightarrow \infty$, the middle parts of the two calculations converge while the head and tail parts tend to be close to unit quaternions with weakening influence, leading to stable results. According to Alexa [2002], the limit exists, so we have

$$\lim_{k \rightarrow \infty} (q_1^{\frac{1}{k}} * q_2^{\frac{1}{k}})^k = \lim_{k \rightarrow \infty} (q_2^{\frac{1}{k}} * q_1^{\frac{1}{k}})^k. \quad (12)$$

For the Trotter product formula

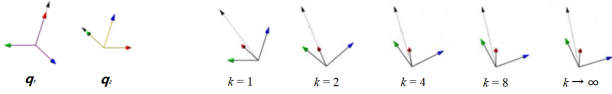
$$e^{A+B} = \lim_{N \rightarrow \infty} (e^{\frac{A}{N}} * e^{\frac{B}{N}})^N, \quad (13)$$

Table 6: Dataset Statistics for ogbl-biokg.

Dataset	Diseases	Drugs	Side Effects	Proteins	Functions	Total Entities	Train Set	Val. Set	Test Set
ogbl-biokg	10687 11.40%	10533 11.23%	9969 10.63%	17499 18.66%	45085 48.08%	93773 100%	4.76M 94%	162k 3%	162k 3%

Table 7: Dimensions and MRR on ogbl-biokg.

Model	Dimension	MRR
TransE	2000	0.7452
RotatE	1000	0.7989
DistMult	2000	0.8043
ComplEx	1000	0.8095
QuatE	500	0.7712
QuatE	1000	0.7954
PairRE	2000	0.8164
AutoSF+	1000	0.8309
AutoSF+	2000	0.8320
APAC _q	500	0.8526
APAC _q	1000	0.8578

Figure 5: Rotations under Different k -sections.

replace $e^{\frac{A}{N}}$, $e^{\frac{B}{N}}$ with $q_1^{\frac{1}{k}}$, $q_2^{\frac{1}{k}}$. With $e^{\log q} = q$, we have

$$\lim_{n \rightarrow \infty} \left(q_1^{\frac{1}{k}} \otimes q_2^{\frac{1}{k}} \right)^k = e^{\log q_1 + \log q_2} \quad (14)$$

(The formal proof of isomorphism between quaternions and matrices is saved for future work). It can be seen that the limit operation is equivalent to find the sum of the logarithms of the two quaternions and compute the exponentiation of the result. The calculation cost is constant. Further extend such operation to a quaternion sequence and we get (4). When the special case of coaxial rotational blending (on the same plane) occurs, the result could be seen as a quaternion formed by adding all rotational angles together.

Illustration. Rotations represented by quaternions q_1, q_2 under different k -sections are shown in Figure 5. The axes in 3D spaces are in red, blue and green respectively and the black arrow is the vector calculated by the axis and the angle. It can be seen that when $k = 8$, the result is close to the result when $k \rightarrow \infty$.

B MODEL TRAINING DETAILS

Experiments are conducted on a Lenovo SR590 server with the hardware configuration including 20 core Xeon * 2

(CPU), 16G * 8 Memory, 1.2TB * 3 SAS disks (in RAID5 mode) and Tesla P100 * 2 (computing cards).

Adam optimizer (Adaptive Estimates of Lower-Order Moments) is adopted and optimal parameters are determined with Grid Search. The hyperparameter pool and optimal parameters could be found on the project homepage. Dropouts are added before and after convolution and after the full connection layer, numbered 1, 2 and 3 respectively. Following Gao et al. (2020), relation-specific biases are applied. The batch normalization strategy is employed to reduce the scaling effect caused by hypercomplex multiplications and control the normalizing rate. It is found that with the batch normalization models converge faster and perform more stable than with the unit quaternion. Early stop strategy is activated when the MRR increase in the last 10 epochs on Val. Set is less than 10-2. In other experiments the optimizer and training strategies are the same unless declared differently.

Author Contributions

Ms. Gao and Ms. Shi help with theretical deduction and verification of the combination of the atrous and circular convolution. Ms. Zhou and Mr. Husen oversee the overall framework and project implementation.

Acknowledgements

The study is supported by the provincial research project in Fujian (FJJKCG20-402).

References

- Marc Alexa. Linear combination of transformations. *ACM Transactions on Graphics (TOG)*, 21(3):380–387, 2002.
- Ivana Balažević, Carl Allen, and Timothy M Hospedales. Hypernetwork knowledge graph embeddings. In *International Conference on Artificial Neural Networks*, pages 553–565. Springer, 2019a.
- Ivana Balažević, Carl Allen, and Timothy M Hospedales. Tucker: Tensor factorization for knowledge graph completion. *arXiv preprint arXiv:1901.09590*, 2019b.
- Antoine Bordes, Nicolas Usunier, Alberto Garcia-Duran, Jason Weston, and Oksana Yakhnenko. Translating em-

- beddings for modeling multi-relational data. *Advances in neural information processing systems*, 26, 2013.
- Zongsheng Cao, Qianqian Xu, Zhiyong Yang, Xiaochun Cao, and Qingming Huang. Dual quaternion knowledge graph embeddings. In *Proceedings of the AAAI Conference on Artificial Intelligence*, volume 35, pages 6894–6902, 2021.
- Ines Chami, Adva Wolf, Da-Cheng Juan, Frederic Sala, Sujith Ravi, and Christopher Ré. Low-dimensional hyperbolic knowledge graph embeddings. *arXiv preprint arXiv:2005.00545*, 2020.
- Linlin Chao, Jianshan He, Taifeng Wang, and Wei Chu. Pairre: Knowledge graph embeddings via paired relation vectors. *arXiv preprint arXiv:2011.03798*, 2020.
- Liang-Chieh Chen, George Papandreou, Iasonas Kokkinos, Kevin Murphy, and Alan L Yuille. Deeplab: Semantic image segmentation with deep convolutional nets, atrous convolution, and fully connected crfs. *IEEE transactions on pattern analysis and machine intelligence*, 40(4):834–848, 2017.
- Rajarshi Das, Arvind Neelakantan, David Belanger, and Andrew McCallum. Chains of reasoning over entities, relations, and text using recurrent neural networks. *arXiv preprint arXiv:1607.01426*, 2016.
- Tim Dettmers, Pasquale Minervini, Pontus Stenetorp, and Sebastian Riedel. Convolutional 2d knowledge graph embeddings. In *Proceedings of the AAAI Conference on Artificial Intelligence*, volume 32, 2018.
- Chang Gao, Chengjie Sun, Lili Shan, Lei Lin, and Mingjiang Wang. Rotate3d: Representing relations as rotations in three-dimensional space for knowledge graph embedding. In *Proceedings of the 29th ACM International Conference on Information & Knowledge Management*, pages 385–394, 2020.
- Haipeng Gao, Kun Yang, Yuxue Yang, Rufai Yusuf Zakari, Jim Wilson Owusu, and Ke Qin. Quatde: Dynamic quaternion embedding for knowledge graph completion. *arXiv preprint arXiv:2105.09002*, 2021.
- Klaus Greff, Rupesh K Srivastava, Jan Koutník, Bas R Steunebrink, and Jürgen Schmidhuber. Lstm: A search space odyssey. *IEEE transactions on neural networks and learning systems*, 28(10):2222–2232, 2016.
- Qingyu Guo, Fuzhen Zhuang, Chuan Qin, Hengshu Zhu, Xing Xie, Hui Xiong, and Qing He. A survey on knowledge graph-based recommender systems. *IEEE Transactions on Knowledge and Data Engineering*, 2020.
- Kelvin Guu, John Miller, and Percy Liang. Traversing knowledge graphs in vector space. *arXiv preprint arXiv:1506.01094*, 2015.
- Yanchao Hao, Yuanzhe Zhang, Kang Liu, Shizhu He, Zhanyi Liu, Hua Wu, and Jun Zhao. An end-to-end model for question answering over knowledge base with cross-attention combining global knowledge. In *Proceedings of the 55th Annual Meeting of the Association for Computational Linguistics (Volume 1: Long Papers)*, pages 221–231, 2017.
- Guoliang Ji, Kang Liu, Shizhu He, and Jun Zhao. Knowledge graph completion with adaptive sparse transfer matrix. In *Thirtieth AAAI conference on artificial intelligence*, 2016.
- Xiaotian Jiang, Quan Wang, Baoyuan Qi, Yongqin Qiu, Peng Li, and Bin Wang. Attentive path combination for knowledge graph completion. In *Asian conference on machine learning*, pages 590–605. PMLR, 2017.
- Rafal Jozefowicz, Wojciech Zaremba, and Ilya Sutskever. An empirical exploration of recurrent network architectures. In *International conference on machine learning*, pages 2342–2350. PMLR, 2015.
- Timothée Lacroix, Nicolas Usunier, and Guillaume Obozinski. Canonical tensor decomposition for knowledge base completion. In *International Conference on Machine Learning*, pages 2863–2872. PMLR, 2018.
- Ni Lao, Tom Mitchell, and William Cohen. Random walk inference and learning in a large scale knowledge base. In *Proceedings of the 2011 conference on empirical methods in natural language processing*, pages 529–539, 2011.
- Yankai Lin, Zhiyuan Liu, Maosong Sun, Yang Liu, and Xuan Zhu. Learning entity and relation embeddings for knowledge graph completion. In *Twenty-ninth AAAI conference on artificial intelligence*, 2015.
- Rui Lu and Zhiyao Duan. Bidirectional gru for sound event detection. *Detection and Classification of Acoustic Scenes and Events*, 2017.
- Farzaneh Mahdisoltani, Joanna Biega, and Fabian Suchanek. Yago3: A knowledge base from multilingual wikipedias. In *7th biennial conference on innovative data systems research*. CIDR Conference, 2014.
- Mojtaba Nayyeri, Xiaotian Zhou, Sahar Vahdati, Reza Izanloo, Hamed Shariat Yazdi, and Jens Lehmann. Let the margin slide for knowledge graph embeddings via a correntropy objective function. In *2020 International Joint Conference on Neural Networks (IJCNN)*, pages 1–9. IEEE, 2020.
- Arvind Neelakantan, Benjamin Roth, and Andrew McCallum. Compositional vector space models for knowledge base completion. *arXiv preprint arXiv:1504.06662*, 2015.

- Dai Quoc Nguyen, Thanh Vu, Tu Dinh Nguyen, and Dinh Phung. Quatre: Relation-aware quaternions for knowledge graph embeddings. *arXiv preprint arXiv:2009.12517*, 2020.
- Maximilian Nickel, Kevin Murphy, Volker Tresp, and Evgeniy Gabrilovich. A review of relational machine learning for knowledge graphs. *Proceedings of the IEEE*, 104(1):11–33, 2015.
- Daniel Ruffinelli, Samuel Broscheit, and Rainer Gemulla. You can teach an old dog new tricks! on training knowledge graph embeddings. In *International Conference on Learning Representations*, 2019.
- Chao Shang, Yun Tang, Jing Huang, Jinbo Bi, Xiaodong He, and Bowen Zhou. End-to-end structure-aware convolutional networks for knowledge base completion. In *Proceedings of the AAAI Conference on Artificial Intelligence*, volume 33, pages 3060–3067, 2019.
- Zhiqing Sun, Zhi-Hong Deng, Jian-Yun Nie, and Jian Tang. Rotate: Knowledge graph embedding by relational rotation in complex space. *arXiv preprint arXiv:1902.10197*, 2019.
- Kristina Toutanova and Danqi Chen. Observed versus latent features for knowledge base and text inference. In *Proceedings of the 3rd workshop on continuous vector space models and their compositionality*, pages 57–66, 2015.
- Théo Trouillon, Johannes Welbl, Sebastian Riedel, Éric Gaussier, and Guillaume Bouchard. Complex embeddings for simple link prediction. In *International conference on machine learning*, pages 2071–2080. PMLR, 2016.
- Shikhar Vashishth, Soumya Sanyal, Vikram Nitin, Nilesh Agrawal, and Partha Talukdar. Interact: Improving convolution-based knowledge graph embeddings by increasing feature interactions. In *Proceedings of the AAAI conference on artificial intelligence*, volume 34, pages 3009–3016, 2020.
- Jingbin Wang, Xiaolian Lai, Jing Lei, and Jingxuan Zhang. Multi-scale dilated convolutional neural network model based on attention mechanism. *Pattern Recognition and Artificial Intelligence*, 2021.
- Quan Wang, Jing Liu, Yuanfei Luo, Bin Wang, and Chin-Yew Lin. Knowledge base completion via coupled path ranking. In *Proceedings of the 54th Annual Meeting of the Association for Computational Linguistics (Volume 1: Long Papers)*, pages 1308–1318, 2016.
- Quan Wang, Pingping Huang, Haifeng Wang, Songtai Dai, Wenbin Jiang, Jing Liu, Yajuan Lyu, Yong Zhu, and Hua Wu. Coke: Contextualized knowledge graph embedding. *arXiv preprint arXiv:1911.02168*, 2019.
- Zhen Wang, Jianwen Zhang, Jianlin Feng, and Zheng Chen. Knowledge graph embedding by translating on hyperplanes. In *Proceedings of the AAAI Conference on Artificial Intelligence*, volume 28, 2014.
- Qizhe Xie, Xuezhe Ma, Zihang Dai, and Eduard Hovy. An interpretable knowledge transfer model for knowledge base completion. *arXiv preprint arXiv:1704.05908*, 2017.
- Bishan Yang, Wen-tau Yih, Xiaodong He, Jianfeng Gao, and Li Deng. Embedding entities and relations for learning and inference in knowledge bases. *arXiv preprint arXiv:1412.6575*, 2014.
- Wenpeng Yin, Yadollah Yaghoobzadeh, and Hinrich Schütze. Recurrent one-hop predictions for reasoning over knowledge graphs. *arXiv preprint arXiv:1806.04523*, 2018.
- Aston Zhang, Yi Tay, Shuai Zhang, Alvin Chan, Anh Tuan Luu, Siu Cheung Hui, and Jie Fu. Beyond fully-connected layers with quaternions: Parameterization of hypercomplex multiplications with $1/n$ parameters. *arXiv preprint arXiv:2102.08597*, 2021a.
- Shuai Zhang, Yi Tay, Lina Yao, and Qi Liu. Quaternion knowledge graph embeddings. *Advances in neural information processing systems*, 32, 2019.
- Yongqi Zhang, Quanming Yao, Wenyan Dai, and Lei Chen. Autosf: Searching scoring functions for knowledge graph embedding. In *2020 IEEE 36th International Conference on Data Engineering (ICDE)*, pages 433–444. IEEE, 2020.
- Yongqi Zhang, Zhanke Zhou, and Quanming Yao. Autosf+: Towards automatic scoring function design for knowledge graph embedding. *arXiv preprint arXiv:2107.00184*, 2021b.
- Peng Zhou, Wei Shi, Jun Tian, Zhenyu Qi, Bingchen Li, Hongwei Hao, and Bo Xu. Attention-based bidirectional long short-term memory networks for relation classification. In *Proceedings of the 54th annual meeting of the association for computational linguistics (volume 2: Short papers)*, pages 207–212, 2016.